VALENTIN POÉNARU

CORRADO TANASI

Representations of the Whitehead manifold Wh^3 and Julia sets

<http://www.numdam.org/item?id=AFST_1995_6_4_3_655_0>

Representations of the Whitehead manifold Wh³ and Julia sets[*]

VALENTIN POÉNARU[1] and CORRADO TANASI[2]

RÉSUMÉ. — Quand on étend à la variété de Whitehead le théorème de représentation pseudo-spine collapsible pour les sphères d'homotopie, les transversales tendues à l'ensemble des lignes doubles présentent un comportement chaotique bien connu. Ce comportement est engendré par une boucle de feedback dynamique qui engendre aussi des ensembles de Julia.

ABSTRACT. — When one extends to the Whitehead manifold the collapsible pseudo-spine representation theorem for homotopy 3-spheres, the tight transversals to the set of double lines present chaotic dynamical behaviour of a very well-known type. This behaviour is generated by a dynamical feedback loop which also generates Julia sets.

KEY-WORDS : Representations of open simply connected 3-manifolds, Whitehead manifolds, tight transversals to the set of double lines, Chaotic behaviour, Julia sets, Mandelbrot set.

AMS Classification : 57 M 30, 58 F 13.

Introduction

The present paper exhibits, posssibly in the simplest form, something which many people expect to happen, namely a connection between wild differential topology in dimension 3 and chaotic behaviour of dynamical systems (see for instance section 6 from [FL]).

The first author has hiven a certain kind of representations for homotopy 3-spheres the so called *collapsible pseudo-spine representations* [Po1]. Subsequently the same author has extended this kind of representations to arbitrary open simply connected 3-manifolds. Completely new features occur in this set up, namely the possibility of infinite accumulation of double points at the source of the representation; we will describe these things in detail later on in the present introduction, but right now let us say already that the point which this present paper makes, is the following. When you try to represent the celebrated Whitehead manifold by the procedure in question and if you take the most natural road for doing so, then the well known Julia sets from the iteration of quadratic polynomials appear very naturally. We will explain these things a bit more in detail. We will briefly review now how the collapsible pseudo-spine representations $K^2 \xrightarrow{f} \Sigma^3$ from [Po1] are generalized. In the present paper we consider an open simply connected 3-manifold V^3, in lieu of Σ^3 and an infinite but locally finite 2-dimensional simplicial complex X in lieu of K^2; this X will be *almost arborescent* (this notion, which we will define precisely later on, is the subtitute for almost-collapsibility in the context of infinite complexes).

With this we will be able to construct a non-degenerate map $X \xrightarrow{f} V^3$ having properties:

(i) The map f is a generic immersion except at a set $\mathrm{Sing}(f) \subset X$ of singularities; but *caution* we will need to leave the simplicial category, fX wil not be a simplicial complex, not even a non-locally finite one, and accordingly f will not be simplicial. But fX will be a *generalized polyhedron*, in a sense which will be made explicit later on; it suffices to say here that the *open regular neighbourhood* $\mathrm{Nbd}(fX) \subset V^3$ continues to be well-defined.

(ii) The double points of f are again commanded by the singularities (with the notation of [Po1] this means that $\Psi(f) = \Phi(f)$). In plain english this also means that if you start zipping away from the singularities, then you catch all the double points.

(iii) The open regular neighbourhood $\mathrm{Nbd}(fX) \subset V^3$ is isotopic to $V^3 - \{$a closed totally discontinous subset which is tame$\}$ (and this will also be made completely explicit later on).

So far we have for V^3 a not completely trivial extension of the (almost-) collapsible pseudo-spine representation theorem for Σ^3, from [Po1].

But now we have a completely new phenomenon; the set of double points of f, i.e. of points $x \in X$ such that $\text{card}(f^{-1}fx) > 1$ which we will denote by $M_2(f) \subset X$ is, generally speaking, *no longer closed* and the main concern of [Po2] and also of the present paper is the study of the *set of limit-points* of $M_2(f)$. In order to get our hands on this set, we will consider the various smooth lines $\Lambda \subset X$ which are *transversal* to $M_2(f)$ and look at the set of limit-points of $\Lambda \cap M_2(f)$, which we denote by $\lim(\Lambda \cap M_2(f))$; here $p \in \lim(\Lambda \cap M_2(f)) \subset \Lambda$ iff there exists an infinite sequence of distinct points $p_1, p_2, \ldots \in \Lambda \cap M_2(f)$ such that $\lim p_n = p$.

Before we go on, some more notations will have to be introduced.

By definition a generalized polyhedron of R^3 is a subspace $Y \subset R^3$ which up to a global diffeomorphism of R^3, can be described as follows. We are given to begin with, a countable (or possibly finite) collection of distinct affine planes $R_1^2, R_2^2, \ldots \subset R^3$ such that $Y \subset \bigcup_i R_i^2$. Moreover our collection of planes has fulfill the following conditions.

(A1) No infinite subcollection of the R_i^2's has a common point.

(A2) There are positive numbers $\varepsilon_1, \varepsilon_2, \ldots$ such that the open subsets $R_1^2 \times (-\varepsilon_1, \varepsilon_1)$, $R_2^2 \times (-\varepsilon_2, \varepsilon_2)$, $\ldots$ of R^3 meet *exactly* like the $R_1^2, R_2^2, \ldots$ In particular this implies that if $p \in R_\alpha^2 \cap R_\beta^2 - R_i^2$ then $\text{dist}(p, R_i^2) > \varepsilon_i$. Also the set of planes $\{R_i^2\}$ is *discrete* in the sense that there ar no "topological relations" (in the space planes of R^3) of the type $\lim_{m=\infty} R_{i_m}^2 = R_{i_0}^2$. Similary, the set of lines $\{R_i^2 \cap R_j^2\}$ and the set of points $\{R_i^2 \cap R_j^2 \cap R_h^2\}$ are also discrete.

(A3) For each R_i^2 we give 2-dimensional piecewise linear submanifold with boundary $L_i^2 \subset R_i^2 \subset R^3$. We will assume these L_i^2's to be of simplest type, like for instance R_i^2 itself, a half plane, a quarter plane or rectangle (possibly with some edges at infinity, or simply deleted). But even in the case when each $p \in Y$ has a neighbourhood in Y which is a locally finite simplicial complex (or, more generally, a neighbourhood which is a closed subset of R^3), $Y \subset R^3$ itself is *not* assumed to be a closed subset.

We do not have to go into more details here and now, since the generalized polyhedra considered in the present paper will be complety explicit.

We consider now in lieu of R^3, a smooth 3-manifold M^3, with $\partial M^3 = \emptyset$. A subset $Z \subset M^3$ will be called a *generalized (sub-)polyhedron of M^3* if locally, i.e. in each coordinate chart $R^3 \subset M^3$, the object $Z \cap R^3$ is a generalized polyhedron in the sense of (A1) to (A3).

We will define now the notion of a *singular generalized polyhedron* which is
locally finite at the source (which we will just call a "singular" locally finite
generalized polyhedron). This is a triple (X, f, M^3) where the following
conditions are fulfilled.

(B1) M^3 is a smooth 3-manifold without boundary, X is a locally finite
simplicial 2-dimensionnal complex and $X \xrightarrow{f} M^3$ is a continous
map which restricted to each simplex of X is a smooth embedding.
The image $fX \subset M^3$ is a generalized subpolyhedron of M^3 (which
also means that, generally speaking, the map f cannot be made
simplicial). We will assume f to be generic.

(B2) There is a closed discrete subset $\text{Sing}(f) \subset X$ which is such that if
$x \in X - \text{Sing}(f)$, then there exists an open neighbourhood $x \in Y \subset
X$ and a smooth coordinate neighbourhood $f(x) \subset R^3 \subset M^3$ such
that $f \mid Y$ is an embedding of Y into R^3. So, outside the discrete
and closed set $\text{Sing}(f)$, f is an immersion.

Caution : Y is a locally finite simplicial complex while $f(Y) \subset R^3$
is generally speaking (although isomorphic, abstractly speaking, to
Y) only a generalized subpolyhedron of R^3.

(B3) For each singularity $\sigma \in \text{Sing}(f)$, we have the admissible local model
from [Po1] (and [Po2]). Explicitely, this means the following (this
is a reminder). For each *singularity* $\sigma \in \text{Sing}(f)$, there are two
rectangles P_1, P_2 of X such that $P_1 \cup P_2 \subset X$ is a neighbourhood
of σ, with the following properties: at the level of X, P_1 and P_2
are *glued together along a common half-line*, the restrictions $f \restriction P_i$
$(i = 1, 2)$ are embeddings, and at the target fP_1 and fP_2 *meet
transversally* (fig. 1.1).

There is a line of double points of f, which starts at the singularity σ.
Such points as we have just described, will be called *undrawable singularities*
(or *admissible singularities*). It is assumed that $f \restriction_{\text{Sing}(f)}$ is injective, and
also that $f(\text{Sing}(f)) \subset M^3$ is a discrete subset which, generally speaking,
need *not be closed*; it is only $\text{Sing}(f) \subset X$ which is closed, at the source. On
the other hand through each singularity $\sigma \in X$ go now exactly two *smooth
sheets* of X, namely P_1 and P_2.

We will say that the *singular generalized polyhedron* X is *arborescent* if
we can obtain it by a sequence of Whitehead dilatations starting with a
point. Also "arborescent" does *not* imply "collapsible" (R^2 for instance is
arborescent). We will say that X is *almost arborescent* if it can be obtained
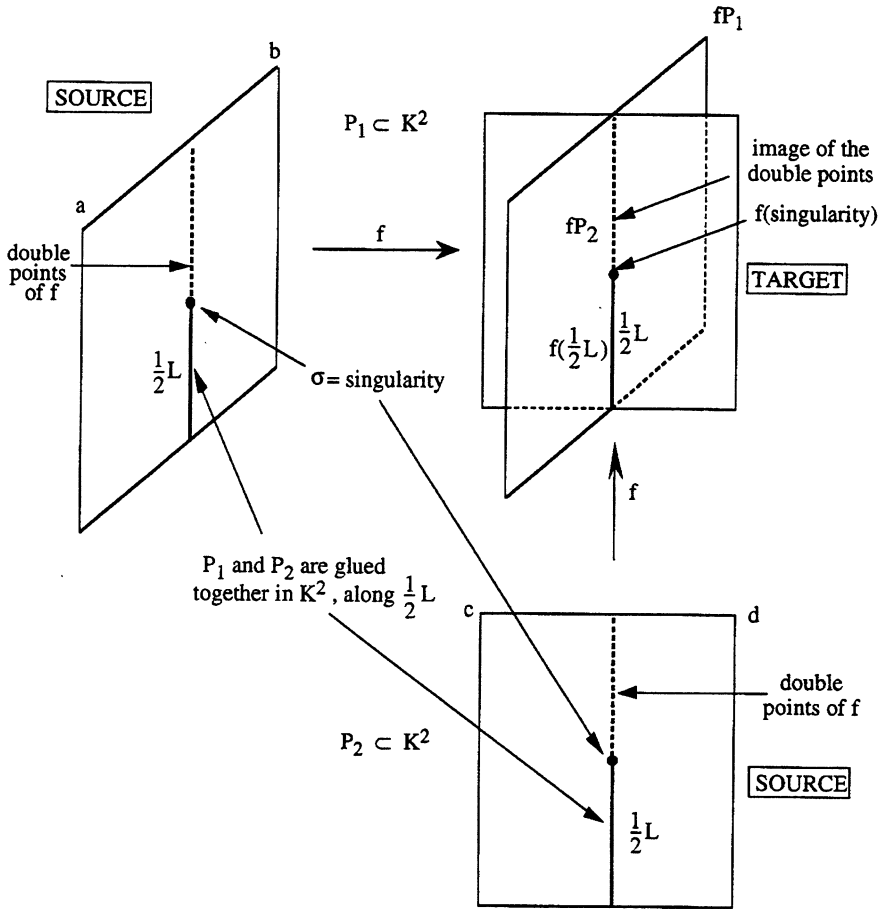
Fig. 1.1 Admissible or "undrawable" singularity.

by a sequence of Whitehead dilatations *and* of additions of 2-cells along their boundaries, starting with a point. In other words, X is *almost arborescent* if it admits an exhaustion by finite simplicial complexes

$$X_0 \subset X_1 \subset \cdots \subset X_n \subset \cdots \subset X_\infty \overset{\text{def}}{=} X \qquad (1.1)$$

such that $X_0 = \{pt\}$ and that each inclusion $X_i \subset X_{i+1}$ is a Whitehead dilatation or the addition of a 2-cell along its boundary.

Let us consider a generalized polyhedron $R^3 \supset Y = \bigcup_i L_i^2$ with quantities $\varepsilon_i > 0$ like in (A2) at the beginning of this section. Consider for every L_i^2 an open tubular neighbourhood of width $\eta_i < \varepsilon_i$, let us call it $L_i^2 \times (-\eta_i, \eta_i)$. The open manifold:

$$\mathrm{Nbd}(Y) = \bigcup_i \left(L_i^2 \times (-\eta_i, \eta_i) \right) \subset R^3 \,,$$

which up to diffeomorphism only depends of $\left(R^3, Y \right)$ is, by definition, the (*open*) *regular neighbourhood* of Y. With this we can define the regular neighoorhood of any :

$$X \xrightarrow{f} M^3 \tag{1.2}$$

as soon as $\mathrm{Sing}(f) = \emptyset$ (i.e. with an immersive f) in particular for generalized polyhedra $Z \subset M^3$.

If V^3 is any *open* 3-manifold, a singular locally finite generalized polyhedron:

$$X \xrightarrow{f} V^3$$

will be called an (*almost*) *arborescent representation* of V^3 which is locally finite "at the source" if the following conditions are fulfilled:

(C1) X is (almost) arborescent.

(C2) $\Psi(f) = \Phi(f)$.

(C3) For the open submanifold $\mathrm{Nbd}(fX) \subset V^3$ there is an isotopy of smooth embeddings $\mathrm{Nbd}(fX) \xrightarrow{i_t} V^3$, where $t \in [\,0\,,1\,]$, such that i_0 is the standard embedding and i_1 is a *diffeomorphism* $\mathrm{Nbd}(fX) \xrightarrow[\approx]{i_1} V^3$.

Remark. — Our i_t is not an ambient isotopy.

For a given open 3-manifold V^3 we will define a type of submanifolds, which we call generically V_h^3 which are defined by :

$$V_h^3 = V^3 - \bigcup_{n=1}^{\infty} C_n \,, \tag{1.3}$$

where the C_n are two-by-two disjoint compact discontinuous tame subsets, not accumulating at finite distance. Up to isotopy, the V_h^3 is uniquely defined once the topological type of $\bigcup_{n=1}^{\infty} C_n$ is determined.

Let $L \subset X$ be a smooth sheet and $\ell \subset L$ a smooth line meeting *transversally* the stratified set $M_2(f) \subset X$. We will say that the *transversal* ℓ is *tight* if we cannot find any 2-cell $D^2 \subset L$ resting with half of its boundary an ℓ and with the other half on a smooth line in $M_2(f)$. In other words, for a *tight transversal* figure 1.2 is forbidden.
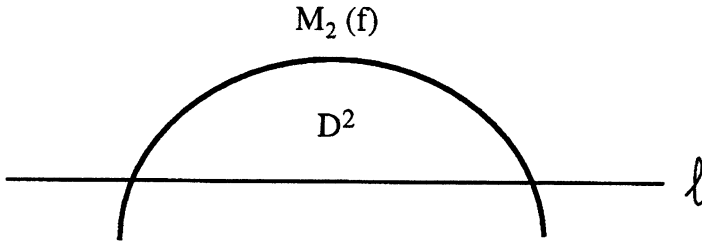
$$M_2\,(f)$$

Fig. 1.2   This figure (supposedly living inside the smooth sheet $L \subset X$) is forbidden for a tight transversal ℓ.

We will only be interested in the following situation as far as singular $X \xrightarrow{f} V^3$'s are concerned. In any sufficiently small smooth sheet $L \subset X$ the set $M_2(f) \cap L$ is a finite union of subsets (actually only one or two), each of them contained in a family $F \subset L$ of "parallel" lines with the following property. For any tight transversal ℓ, the set $F \cap \ell$ is discrete, i.e. $F \cap \lim(F \cap \ell) = \emptyset$ (this behaviour is at the opposite pole with respect to laminations).

All this having been said we can state now the following theorem which is proved in [Po2] and which gives the general context for this paper. What we will call the *representation theorem* below is actually only part of the theorem proved in [Po2] but this part is the only relevant one for this context. So here is the theorem.

REPRESENTATION THEOREM .— *Let V^3 be an open simply connected 3-manifold. We can always find a V_h^3 (like in (1.3)) and a locally finite almost arborescent representation of V_h^3*

$$X \xrightarrow{f} V_h^3 \subset V^3 \tag{1.4}$$

with the following property.

For any tight precompact transversal $\ell \subset X$ the limit set of $M_2(f) \cap \ell$, i.e.

$$\lim(M_2(f) \cap \ell) \subset \ell$$

is finite.

This statement should be compared with the following.

(ALMOST) COLLAPSIBLE PSEUDO-SPINE REPRESENTATION THEOREM
(see [Po1]) . — *Let Σ^3 be a homotopy 3-sphere. We can always find a
finite (non-void) set $E \subset \Sigma^3$ and an (almost) collapsible representation of
$\Sigma^3 - E$:*

$$K^2 \xrightarrow{g} \Sigma^3 - E .$$

(Here K^2 is a bona fide finite simplicial complex and g a non-degenerate
simplicial map.)

We will make now a few comments, first about the representation theorem
itself. In some sense this theorem is the best possible, since one can
prove the following fact. If $X \xrightarrow{f} V_h^3 \subset V^3$ is like in the representation
theorem and such that for any tight transversal $\lim(M_2(f) \cap \ell) = \emptyset$ (i.e.
$\text{card}(M_2(f) \cap \ell) < \infty$) then $\pi_1^\infty V^3 = 0$. This fact is proved, among other
things, in [Po2]. Only tight precompact transversals will be considered.

Now the representation (1.4) is, generally speaking, *highly redundant* in
the sense that any a given double point

$$(x, y) \in M^2(f) \subset X \times X$$

of the map f can be reached in many distinct ways, via zippings starting
from the singularities of f. Very much linked with this redundancy is the
fact that in order to get the *finitenes* condition for our almost arborescent
representation, we had to go from V^3 to V_h^3 thereby (highly) increasing
the second homotopy group π_2. In the same spirit, when we realize f by
elementary $O(i)$ moves [Po1], many of these will be $O(3)$'s and each of these
creates a new π_2-generator.

In Theorem A below we consider a *non-redundant* representation of the
classical Whitehead manifold and what we find is that if this representation
"is the simplest possible" (that is what (c) in Theorem A is supposed
to tell us), then there are tight transversals ℓ such that $\lim(M_2(f) \cap \ell)$
is uncountable (it actually exhibits chaotic behaviour). To put things
slightly differently, a high redundancy is very likely *unavoidable for a wild
3-manifold* V^3 (with $\pi_1^\infty V^3 \neq 0$ like the Whitehead manifold), if one insists
in getting an (almost) arborescent representation satisfing the *finiteness*
property from the *representation theorem* above. It will turn out that the
set $M_2(f) \cap \Lambda$, where Λ is a certain tight transversal, is generated by a
dynamical feedback loop which is the same as the one which generates

the Julia set of a quadratic polynomial which has the property that under iteration the unique critical point escapes to infinity. In other words again, the *finiteness* property in our representation theorem is achieved only at the price of a lot of *redundancy*.

As far as the representation theorem itself is concerned, it is part of a general approach developed by the first author in connection with the problem of the simple connectivity at infinity for the universal covering space $\widetilde{M}^3$ of a closed 3-manifold M^3, and our Theorem A is an addendum to the representation theorem in question; but it is *not* part of the approach to the proof of $\pi_1^\infty \widetilde{M}^3 = 0$.

Before we can state our result we have to open another parenthesis. We will consider a real quadratic polynomial f_λ which is such that iterates of the unique critical point go to infinity. We consider also a certain set of cardinality two $E = \{x_0, y_1\} \subset R$ (fig. 2.1) and for this set we consider the set

$$E \cup f_\lambda^{-1} E \cup f_\lambda^{-2} E \cup \cdots \subset [\, 0\,, 1\,].$$

As we will see in the next section, the set of limit points of $E \cup f_\lambda^{-1} E \cup f_\lambda^{-2} E \cup \cdots$ is the Julia set (see for instance [B]) of the quadratic polynominal f_λ.

The goal of the next section of this paper is to exhibit the following fact which we believe to reflect a general kind of a pattern and which we will call.

THEOREM A.— *We cas find an arborescent representation, which is locally finite at the source, of the Whitehead manifold* Wh^3.

$$K \xrightarrow{g} \text{Wh}^3\,,$$

with the following features:

(a) *We will have*

$$K = D_0 \cup D_1 \cup D_2 \cup \cdots$$

where each D_i is a 2-disk, for every i the disks D_{i-1} and D_i are glued together along a common arc and, in K, these arcs are two-by-two disjoined.

(b) *The map g has no triple points, each connected component of $M_2(g)$ is a finite tree starting at a singular point, and for each tight transversal ℓ we have*

$$M_2(g) \cap \big(\lim \big(M_2(g) \cap \ell\big)\big) = \emptyset\,.$$

(c) *Each $g(\partial D_i)$ is the middle curve $S^1 \times pt \subset S^1 \times D^2 = T_i$ of the i'th solid torus T_i of Wh^3, $g(D_i) \subset Int\ T_{i+1}$ and $g(D_i)$ is a spine of T_{i+1}.*

(d) *We can find a tight transversal $\Lambda \subset D_0$ to $M_2(g)$ with a disjoined partition*

$$\Lambda \cap M_2(g) = \sum_{i=1}^{\infty} \underbrace{\{double\ points\ involing\ D_0\ and\ D_i\}}_{call\ this\ F_i} \subset [\,0\,,\,1\,].$$

so that there is an order preserving bijective map

$$E \cup f_\lambda^{-1}(E) \cup f_\lambda^{-2}(E) \cup \cdots \xrightarrow{\varphi} \Lambda \cap M_2(g)$$

which sends $f_\lambda^{-n} E$ onto F_{n+1}.

(e) *The set of limit points of $\Lambda \cap M_2(g)$ is a Cantor set, actually it is the Julia set the polynomial f_λ.*

The following section owes a lot to the friendly help of John Hamal Hubbard who showed the first author how his algorithms concerning double points fitted into the context of the Julia sets.

2. Whitehead and Julia algorithms

The point we are trying to make in the present section is the following. As already said , the *finitess* in the representation theorem quoted in the introduction to this paper (and which is proved in [Po2]) was achieved at the cost of a lot *redundancy* (i.e. by going from V^3 to V_h^3). We will show here that for the simplest possible representation of the Whitehead manifold Wh^3 (i.e. for a non-redundant representation of a wild simply-connected open 3-manifold), the set of limit points of double points, on a transversal to the double lines exhibits *chaotic behaviour*, in fact a chaotic dynamical behaviour of a very well-know type.

But before we can state exactly our result we need to recall a number of facts about holomorphic dynamics. Consider a (real) quadratic polynomial $f_\lambda(x) = \lambda x(1-x) - \mu$ (with a fixed small $\mu > 0$) with the parameter value $\lambda > 0$ fixed in such a way that the sequence of iterates of the (unique) critical point of f_λ is *unbounded*. Figure 2.1 shows the graph of such a f_λ (with $\lambda = 6.185$ and $\mu = 0.5$); in this figure the critical point of f_λ is $x = 1/2$ and as we can see, by iterating,
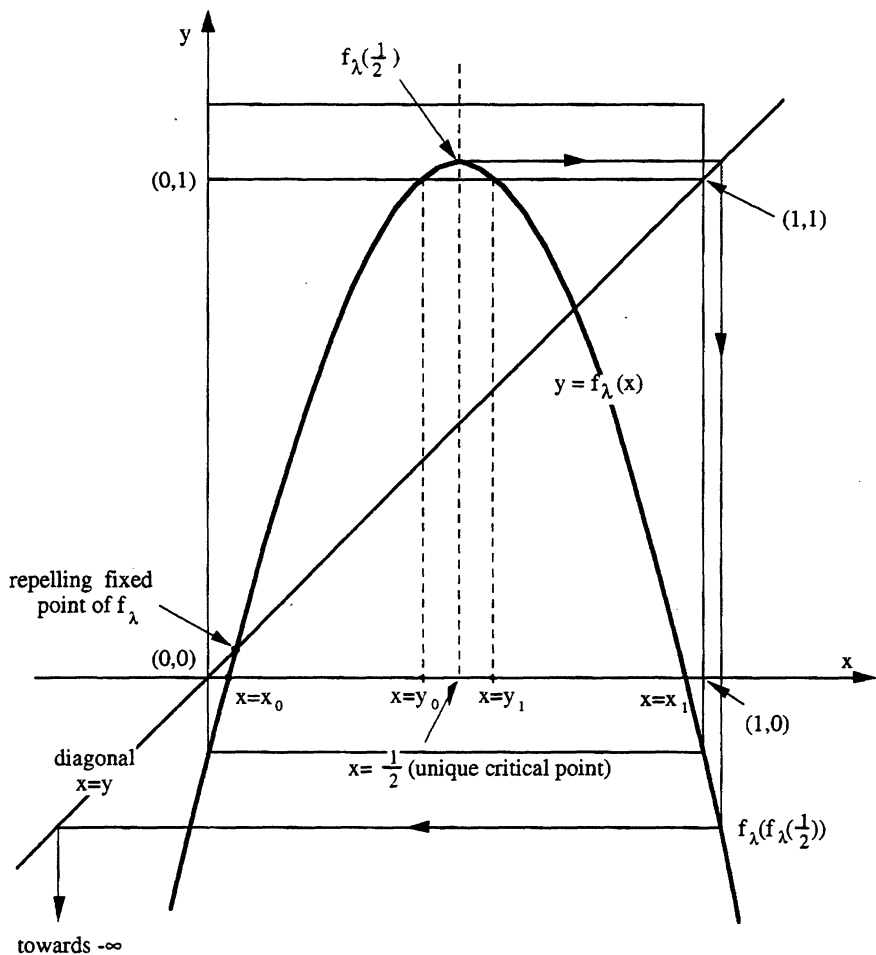
Fig. 2.1 The iterates of the unique critical point of f_λ escape to infinity.

$$f_\lambda\left(\frac{1}{2}\right), \; f_\lambda\left(f_\lambda\left(\frac{1}{2}\right)\right), \; f_\lambda\left(f_\lambda\left(f_\lambda\left(\frac{1}{2}\right)\right)\right), \; \ldots$$

we get an unbounded sequence. If we let things become complex, rather than real, and go to the $P_c(z) = z^2 + c$ representation then one defines in general $J_c = \{\text{the filled Julia of } P_c(z)\}$ where $J_c = \{\text{the set of } z\text{'s such that } P_c^n(z) \text{ stays bounded}\}$ and the Mandelbrot set $M = \{\text{those } c\text{'s which are such that } c \in J_c\}$. (Note that while J_c lives in the complex z-plane, M lives in the c-plane.) One also shows that $c \in M$ if and only if J_c is

connected. One defines the Julia set as ∂J_c but outside at the Mandelbrot set $\partial J_c = J_c = \{$a Cantor set$\}$. Our polynomials (fig. 2.1) correspond to those real values of c living outside the Mandelbrot set in the open half-line contained between $-\infty$ and M (see [B]).
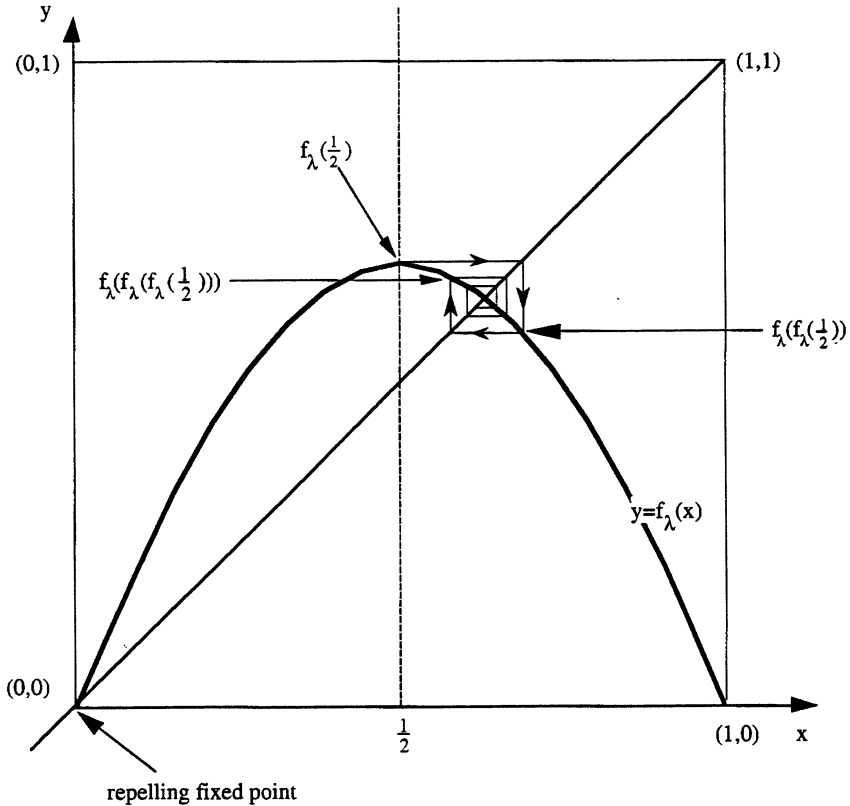

Fig. 2.2 Here the iterates of the critical point of f_λ do not escape to infinity but are trapped at finite distance by an attractor.

For the Julia set J_λ of our f_λ (fig. 2.1) we can take any of the following equivalent definitions.

(α) The Julia set J_λ is the set of limit points of

$$E \cup f_\lambda^{-1}(E) \cup f_\lambda^{-1}\left(f_\lambda^{-1}(E)\right) \cup f_\lambda^{-1}\left(f_\lambda^{-1}\left(f_\lambda^{-1}(E)\right)\right) \cup \cdots$$

for any finite set $E \subset R$.

(β) If, in terms of figure 2.1, we think of f_λ as being a *not everywhere well-defined* map $[0,1] \to [0,1]$, then our $J_\lambda \subset [0,1]$ is exactly the subset where all the iterates of f_λ are well-defined.

(γ) The Julia set J_λ is the subset of the complex z-plane ($z = x + iy$) which is such that if $z_0 \in J_\lambda$ then there is *no* neighbourhood N of z_0 such that, when restricted to $z \in N$, the set of iterates of $f_\lambda(z)$ is a normal family. In other words this is the *chaotic set*, as far as f_λ is concerned.

(δ) J_λ is also the set of points the iterates of which do not escape to infinity (which, of course, is another way to say that the action of f_λ on this set is chaotic).

It is a weel-known fact that J_λ is a Cantor set for any polynomial f_λ which is like in figure 2.1 and as long as this is so, all those J_λ's are the same object, up to a quasi-conformal homeomorphism of complex plane. By constrast with what we see in figure 2.1, the f_λ from the figure 2.2 has a connected "filled" Julia set and it corresponds to a value of the parameter living in the Mandelbrot set M (unlike our f_λ).

For more details about all these things, one can consult [B] or any other standard reference on this subject.

Remark. — The dynamical behaviour displayed in figure 2.1 is very much related to the Smale horseshoe [S] (unlike the more subtle dynamics from figure 2.2, which is connected to the Feigenbaum cascade of period-doublings and transition to chaos [B], [F]). But for the discussion which follows the Julia set standpoint seems more natural than the horseshoe description; we will see this very soon.
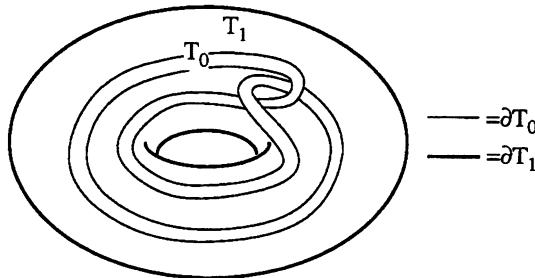

Fig. 2.3

In the figure 2.1 we can see two points x_0, y_1 which are such that $f_\lambda(x_0) = 0$, $f_\lambda(y_1) = 1$, the value x_0 being chosen as small as possible while y_1 is as large possible. We will denote $E = \{x_0, y_1\}$ and consider the set

$$\mathcal{E} \stackrel{\text{def}}{=} E \cup f_\lambda^{-1} E \cup f_\lambda^{-2} E \cup f_\lambda^{-3} E \cup \cdots \subset [\, 0 \, , 1 \,]. \qquad (2.1)$$

As already said before the set of limit points of $\mathcal{E}$ is the Julia set of our f_λ. Let us consider now some arc Λ and a countable subset $\mathcal{F} \subset \Lambda$ endowed with a disjoined partition into finite subsets

$$\mathcal{F} = F_1 \cup F_2 \cup F_3 \cup \cdots \subset \Lambda. \qquad (2.2)$$

We will say that the partition (2.2) *obeys to the Julia algorithm* if there is an order preserving bijective map sending $\mathcal{F}$ onto $\mathcal{E}$ in such a way that for each n we have $\varphi(F_{n+1}) = f_\lambda^{-n} E$. All this having been said, we consider now the simplest Whitehead manifold Wh^3 [R], which is obtained by iterating the embedding $T_0 \subset T_1$, or more explicitely

$$\{\text{solid torus of genus one}\} = T_0 \subset \mathrm{Int}\, T_1 \subset T_1 = \{\text{solid torus} \\ \text{of genus one}\}$$

from figure 2.3 (with null-framing). It is a well-know fact that for the open contractible 3-manifold Wh^3 we have $\pi_1^\infty \mathrm{Wh}^3 \neq 0$.

The goal of this section is to prove the theorem A from the introduction, which we restate below in a slightly modified form.

THEOREM A. — *We can find an arborescent representation of the Whitehead manifold* Wh^3

$$K \xrightarrow{g} \mathrm{Wh}^3 \,,$$

with the following features:

   (1) (Reminder) The space K is a locally finite simplicial complex which can be obtained starting with a point, by an infinite sequence of Whitehead dilatations (which is itself locally finite).

   (2) Actually we will have

$$K = D_0 \cup D_1 \cup D_2 \cup \cdots$$

   where each D_i is a 2-disk, for every i the disks D_{i-1} and D_i are glued together along a common arc and, in K, these arcs are two-by-two disjoined.

(3) *The map g has no triple points and each connected component of $M_2(g)$ is a finite tree, starting at a singular point. Moreover, for any tight transversal ℓ to the $M_2(g)$ we have $M_2(g) \cap \lim(M_2(g) \cap \ell) = \emptyset$.*

(4) *(This point, which will be explained in much more detail, later on, is supposed to tell us that $K \xrightarrow{g} Wh^3$ is the simplest possible representation of Wh^3). Each $g(\partial D_i)$ is the middle curve $S^1 \times pt \subset S^1 \times D^2 = T_i$ of the i'th solid torus T_i of Wh^3, $g(D_i) \subset \mathrm{Int}\, T_{i+1}$ and $g(D_i)$ is a spine of T_{i+1} (fig. 2.3.1).*

(5) *We can find a tight transversal $\Lambda \subset D_0$ to $M_2(g)$ with a disjoined partition*

$$\Lambda \cap M_2(g) = \sum_{i=1}^{\infty} \underbrace{\{double\ points\ involving\ D_0\ and\ D_i\}}_{we\ call\ this\ F_i} \subset [\,0\,,1\,]. \quad (2.3)$$

so that there is an order preserving bijective map sending $f_\lambda^{-n} E$ onto F_{n+1}

$$E \cup f_\lambda^{-1}(E) \cup f_\lambda^{-2}(E) \cup \cdots \xrightarrow{\varphi} \Lambda \cap M_2(g)$$

and hence (2.3) obeys the Julia algorithm.

(6) *The set of limit points $\Lambda \cap M_2(g)$ is a Cantor set, it is actually the Julia set the polynomial f_λ.*

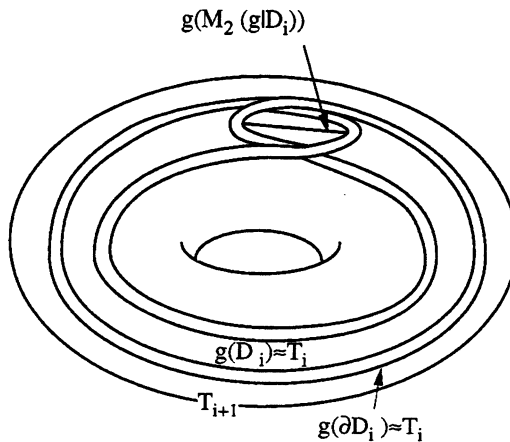**All these things will be looked at in detail in the rest of this section**

Fig. 2.3.1 $g(D_i) \diagup T_{i+1}$, i.e. $g(D_i)$ is a spine of T_{i+1}.

LEMMA 2.1.— *There is an arborescent representation of the Whitehead manifold* Wh^3

$$K \xrightarrow{g} \mathrm{Wh}^3 \tag{2.4}$$

which is such that g has no triple points.

Proof.— We will explicitly construct such a $K \xrightarrow{g} \mathrm{Wh}^3$ which in some sense is the simplest possible one, before analyzing its further features. But it will be easier to start with another representation

$$K_1 \xrightarrow{g_1} \mathrm{Wh}^3 \tag{2.5}$$

Which is *not* arborescent any longer, but which still has the following properties.

(a) The space K_1 is a locally finite contractible simplicial complex; but this K_1 will not be *arborescent* (i.e. it is no longer obtainable from a point, via Whitehead dilatations). We also have $M_3(g_1) = \emptyset$. The next three points are just a reminder.

(b) Except for admissible singularities like the ones in figure 1.1, g_1 is a generic immersion without triple point.
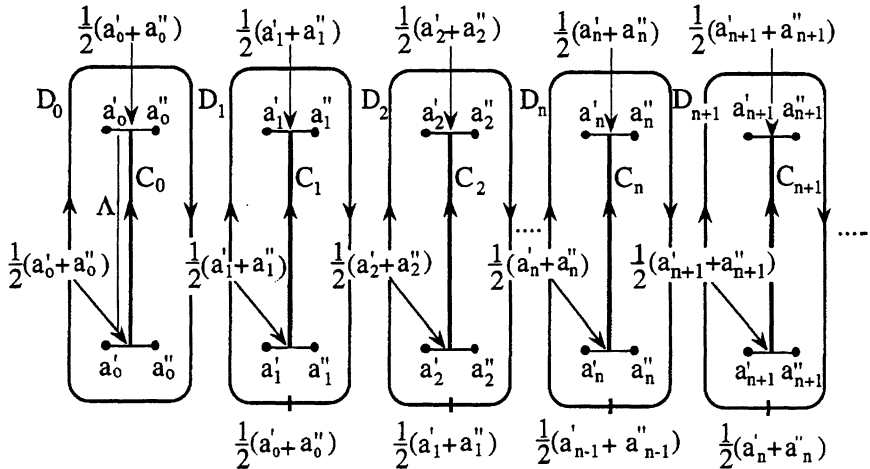

Fig. 2.4 K_1 is a quotient space of the disjoined union $\sum_0^\infty D_n$ and points of $\sum_0^\infty D_n$ with the same image in K_1 carry the same letters in this figure.

(c) We have $\Psi(g_1) = \Phi(g_1)$.

(d) The subset $g_1 K_1 \subset \mathrm{Wh}^3$ is a *non-singular generalized polyhedron* and there is an (improper, i.e. non-ambient) isotopy of

$$\mathrm{Nbd}(g_1 K_1) \xrightarrow{i_0} \mathrm{Wh}^3$$

changing it into a diffeomorphism $\mathrm{Nbd}(g_1 K_1) \approx \mathrm{Wh}^3$.

We will eventually get our (2.4) by a very easy pertubation of the simpler object (2.5). From a purely abstract viewpoint (i.e. if we forget the map g_1), the space K_1 will be obtained by glueing together infinitely many copies of the 2-disk, namely $D_0, D_1, D_2, \ldots$, (fig. 2.4). We actually will have to quotient the D_i's before glueing them together.
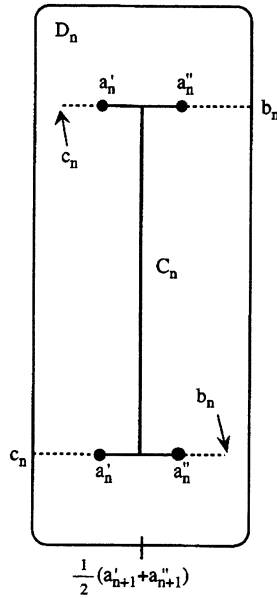

Fig. 2.5 $M_2(g_1 \mid \overline{D}_n)$; the double points are dotted; also $\bullet$ = singularity; this figure is at the source of the map g_1.

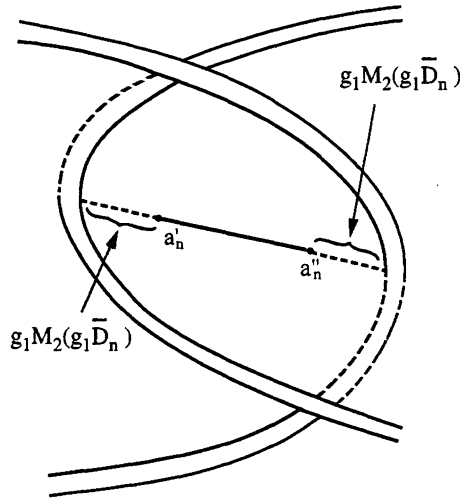The quotient and glueing pattern is the following (see again fig. 2.4).

Fig. 2.5.a   This figure which is at the target corresponds to figure 2.5;
the fat arc $[a'_n, a''_n]$ is not a double line;
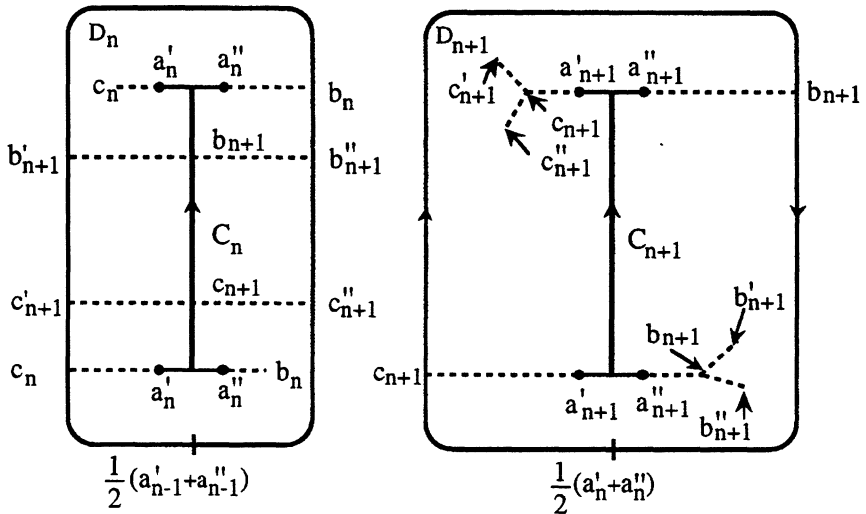the a'_n, a''_n are undrawable singularities

Fig. 2.6 $M_2\big(g_1 \mid (\overline{D}_n \cup \overline{D}_{n+1})\big).$

To begin with, at the level of each D_n (for $n = 0, 1, 2, \ldots$) we identify (in the orientable fashion) the two copies of the arc $[a'_n, a''_n]$ which are contained in the interior of D_n.
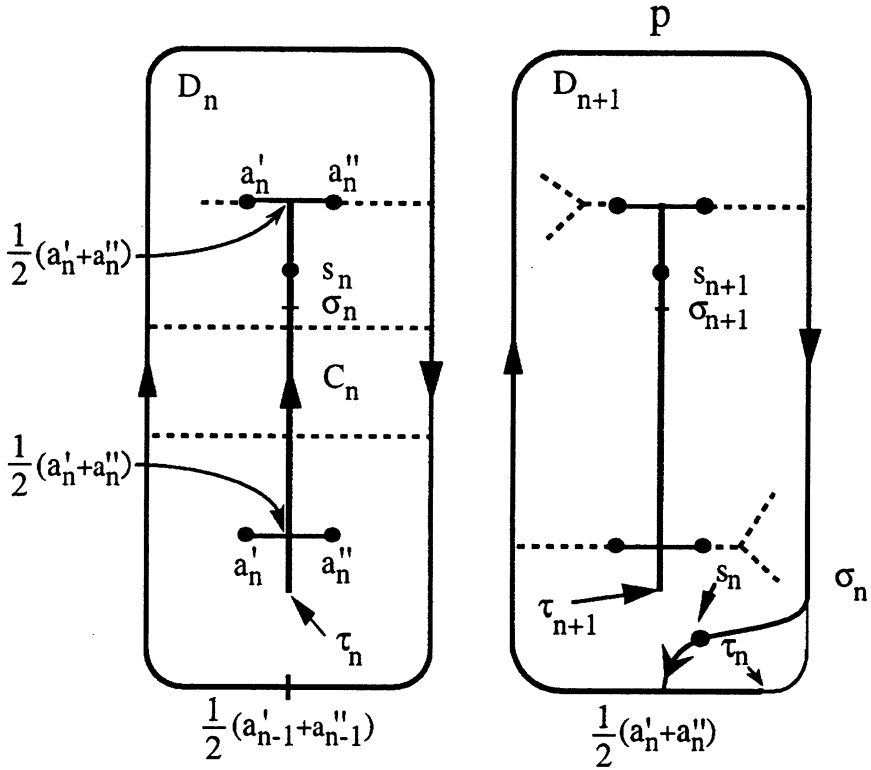

Fig. 2.7 $\overline{D}_n \cup \overline{D}_{n+1} \subset K_2$ and $M_2\big(g_2 \mid (\overline{D}_n \cup \overline{D}_{n+1})\big) = M_2\big(g_1 \mid (\overline{D}_n \cup \overline{D}_{n+1})\big)$;
the points s_n, s_{n+1} are not yet singular;
they will become so at the level of K (fig 2.8).

It is understood that the two middle points $(1/2)(a'_n + a''_n)$ are glued together in this process. Let us denote by $\overline{D}_0, \overline{D}_1, \overline{D}_2, \ldots$ the quotient spaces of $D_0, D_1, D_2, \ldots$ obtained in this way. The image of the arc $C_n \subset D_n$ (which joins the middle points of the two arcs $[a'_n, a''_n]$) becomes a circle, which we denote by the same letter $C_n \subset \overline{D}_n$.
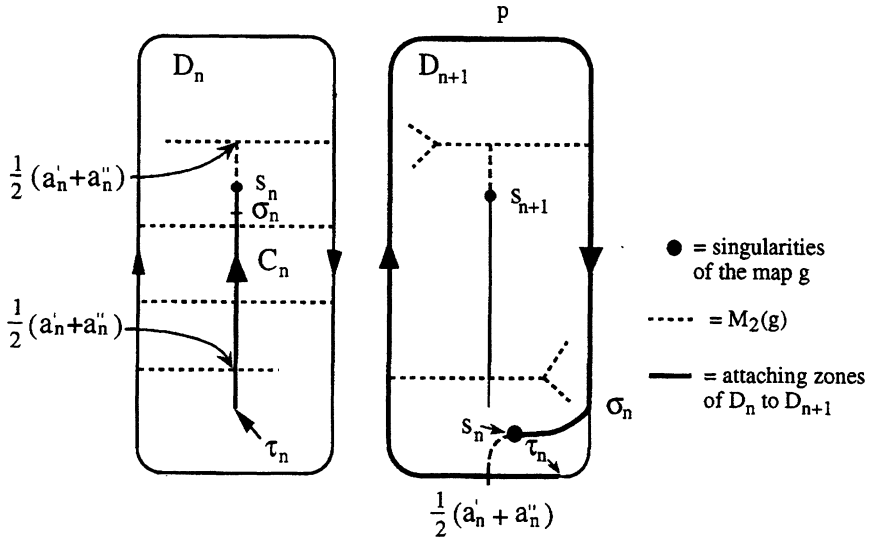
Fig. 2.8 $D_u \cup D_{n+1} \subset K$; all the dotted lines are double points of g; they include $M_2\big(g \mid (D_n \cup D_{n+1})\big)$, but they are far from exhausting $M_2(g) \cap \big(D_n \cup D_{n+1}\big)$, as we shall see explicitly later on.

Notice that $\partial \overline{D}_p = \partial D_p$. Next we glue for each $n+1$ ($n = 0, 1, \ldots$) the boundary $\partial \overline{D}_{n+1} = \partial D_{n+1}$ to the circle $C_n \subset \overline{D}_n$ via a homeomorphism. In terms of figure 2.4 it will be assumed (in order to make things precise) that the arrows of C_n and ∂D_{n+1} correspond to each other. The result of this operation is our $K_1 = \overline{D}_0 \cup \overline{D}_1 \cup \cdots$, which will be the source of the map g_1.

Consider now the sequence of embedded solid tori of genus one, each one inside the interior of the next, which defines Wh^3

$$T_0 \subset T_1 \subset T_2 \subset \cdots \subset T_n \subset \cdots \subset \mathrm{Wh}^3 . \qquad (2.6)$$

The map $K_1 \xrightarrow{g_1} \mathrm{Wh}^3$ will be subjected to the following list of conditions.

Conditions on g_1

(0) The image of $\partial \overline{D}_n \subset K_1$ is contained in Int T_n and $g_1 \partial \overline{D}_n \subset T_n$ is a spine of T_n.

(1) The image of $\overline{D}_n \subset K_1$ is contained in Int T_{n+1} and $g_1 \overline{D}_n \subset T_{n+1}$ is a spine of T_{n+1}.

(2) The double points of the map $g_1 \mid \overline{D}_n$ are like in figure 2.5 and the singularities of g_1 are exactly

$$\text{Sing}(g_1) = \left\{ a'_0, \, a''_0, \, a'_1, \, a''_1, \, \ldots, \, a'_n, \, a''_n, \, \ldots \right\} \subset K_1 \,.$$

In figure 2.5 (and also in figure 2.6) we use the convention that points on the dotted lines denoted with the same letter (like b_n, c_n, ...) are identified to each other via the map $K_1 \xrightarrow{g_1} \text{Wh}^3$.

(3) The set $g_1 \overline{D}_n$ is very thin with respect to $g_1 \overline{D}_{n+1}$ for each n; in more precise terms $g_1 \overline{D}_n$ is concentrated inside a thin tubular neighbourhood of $g_1 \partial \overline{D}_{n+1}$ and the double points of $g_1 \mid (\overline{D}_n \cup \overline{D}_{n+1})$ are like in figure 2.6.

These conditions still leave a lot of margin of maneuver but they completely determine the subset $M_2(g_1) \subset K_1$ modulo a *not necessarily ambient isotopy*. (Our "margin of maneuver" allows for an arbitrary reparametrization of the source, and also for an arbitrary non-ambient isotopy of the image $g_1 K_1 \subset \text{Wh}^3$ inside the target.) We will make this set $M_2(g)$ completely explicit later on. It should be abvious that $M_2(g_1)$ is acyclic and with $M_3(g_1) = \emptyset$. Moreover $\text{Nbd}(g_1 K_1) \subset \text{Wh}^3$ is completely determined modulo an isotopy of embeddings which is not ambient; proprieties (a), (b), (c), (d) are satisfied. It will be convenient to change $K_1 \xrightarrow{g_1} \text{Wh}^3$ into a variant $K_2 \xrightarrow{g_2} \text{Wh}^3$ before our real $K \xrightarrow{g} \text{Wh}^3$ can be defined. In going from K_1 to K_2 we keep the same principle $K_2 = \overline{D}_0 \cup \overline{D}_1 \cup \overline{D}_2 \ldots$ but *the glueing pattern of $\overline{D}_n$ to $\overline{D}_{n+1}$ will be slightly different*. In terms of figure 2.7, $C_n \subset \overline{D}_n$ will be identified now with the curve

$$\left[\frac{1}{2} \left(a'_n + a''_n \right), \, p \,, \, \sigma_n \,, \, \frac{1}{2} \left(a'_n + a''_n \right) \right]$$

contained in $\overline{D}_{n+1}$ and which coincides with $\partial \overline{D}_{n+1} = \partial D_{n+1}$ *except for the small arc*

$$\left[\sigma_n \,, \, s_n \,, \, \frac{1}{2} \left(a'_n + a''_n \right) \right]$$

which is close to the arc

$$\left[\sigma_n \,, \, \tau_n \,, \, \frac{1}{2} \left(a'_n + a''_n \right) \right] \subset \partial \overline{D}_{n+1}$$

but sits in the interior. Also the arc [the lower $(1/2)(a'_n + a''_n), \tau_n] \subset \overline{D}_n$ is glued now to $[(1/2)(a'_n + a''_n), \tau_n] \subset \partial \overline{D}_{n+1}$. It is understood that the arc

$$\left[\sigma_n \,, \, s_n \,, \, \text{the upper} \frac{1}{2} \left(a'_n + a''_n \right) \right] \subset C_n \subset \overline{D}_n$$

is very short so that the passage $K_1 \Rightarrow K_2$ is far from the double points of the map g_1. The double points of g_2 are rigorously the same as those of g_1. One finally gets (K, g) from (K_2, g_2) by keeping fixed the image $g_2 K_2 = gK \subset \mathrm{Wh}^3$ but by unglueing K_2 along each tripod

$$\left[s_n ; \text{ upper } \frac{1}{2} (a'_n + a''_n) ; a'_n, a''_n \right] \quad \text{for } n = 0, 1, 2, \dots$$

So, in passing from (K_2, g_2) to (K, g), figure 2.7 changes into 2.8. The arc $[\tau_n, \sigma_n, s_n] \subset D_n$ is glued now isomorphically (at the level of K) to the fat curve $[\tau_n, p, \sigma_n, s_n] \subset D_{n+1}$ for $n = 0, 1, 2, \dots$ and *this defines the space K which is arborescent*. This K is again a quotient of $\bigcup_0^\infty D_n$ but now each D_n injects into K. The pair of singularities a'_n, a''_n is replaced by the unique singularity s_n and we continue to have $M_3(g) = \emptyset$ (the lower $(1/2)(a'_n + a''_n) \in D_n$ continues to be glued to $(1/2)(a'_n + a''_n) \in D_{n+1}$ at the source of g). This finishes the description of $K \xrightarrow{g} \mathrm{Wh}^3$.

Rermarks

(A)   The double point structures of g and $g_1(g_2)$ differ only in the neighbourhood of s_n ($n = 0, 1, 2, \dots$. In particular, in the neighbourhood of $\left[\text{lower } (1/2)(a'_n + a''_n), \sigma_n\right] \subset C_n$, the double points of g and of g_1 are exactly the same.

(B)   The construction of $(K \xrightarrow{g} \mathrm{Wh}^3)$ leaves a lot of margin of maneuver; actually exactly the same as for $(K_1 \xrightarrow{g_1} \mathrm{Wh}^3)$. We will give now.

The algorithm which generates the transverse structure $M_2(g) \subset K$

We will consider in D_0 a line Λ parallel to the $\left[\text{lower } (1/2)(a'_0 + a''_0), \sigma_0\right]$ (see the left side of figure 2.7, with $n = 0$) and which is slightly shorter than our $\left[(1/2)(a'_0 + a''_0), \sigma_0\right]$. This line which is contained inside the smooth part of K is a transversal to $M_2(g)$ which is tight with respect to $M_2(g)$ and it is disjoint from $M_2(g \mid D_0)$. Moreover our *tight transversal* Λ (which we can also see in figure 2.4) is supposed to be long enough so that it meets (exactly once) every arc in
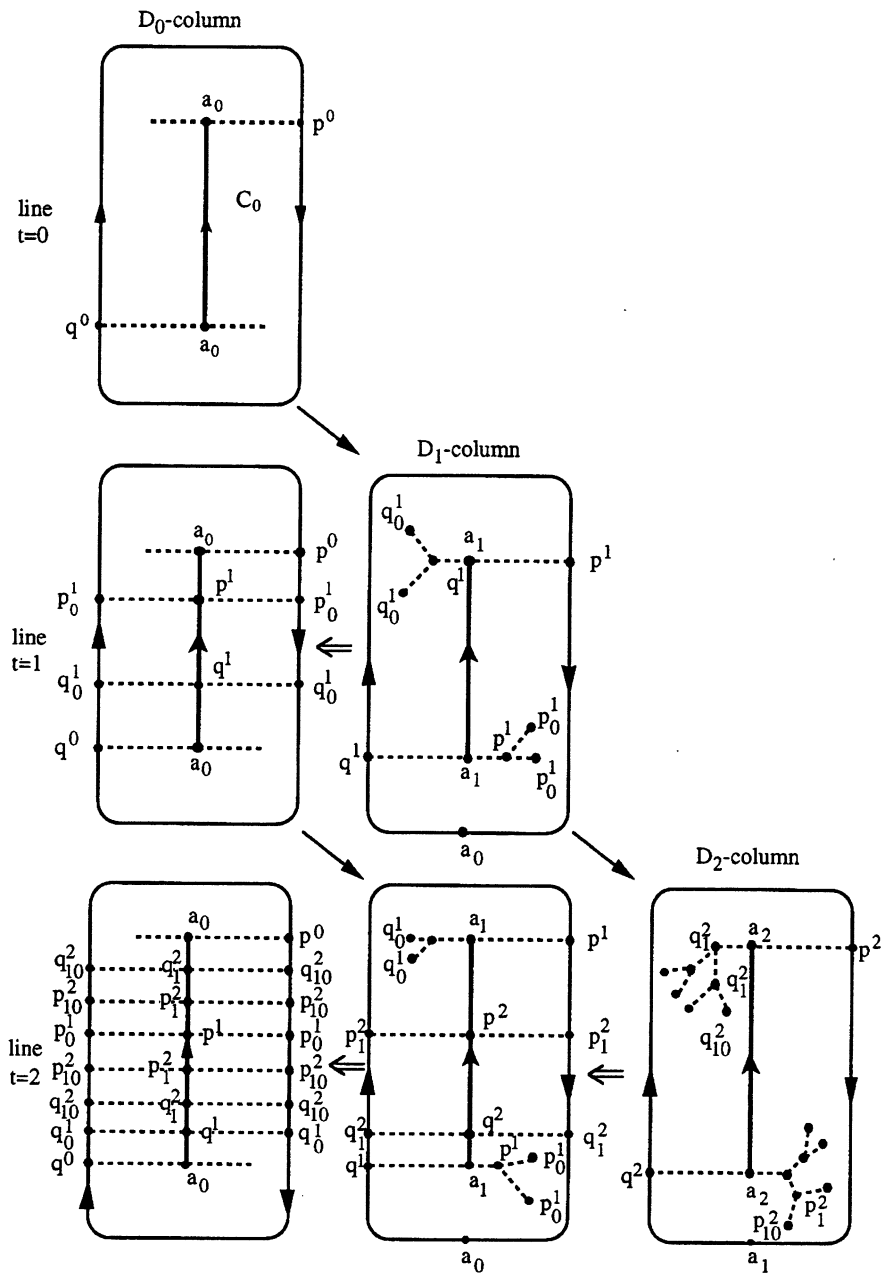
$$M_2(g) \cap D_0 - M_2(g \mid D_0). \tag{2.7}$$

Fig. 2.9   This figure (next page) and figure 2.9b) which continues it shows the recursive rules for building $M_2(g_1) \subset K_1$; to simplify matters we made as if

$$a'_n = a''_n = (1/2)(a'_n + a''_n) \overset{\text{def}}{=} a_n, \ n = 0, 1, 2, \dots;$$

the double points appear as dotted lines and we are really interested in what happens with $\mathrm{Int} \, C_0 \cap M_2(g_1) \approx \Lambda \cap M_2(g)$.

Representations of the Whitehead manifold Wh^3 and Julia sets

D_0-column

a_0
p^0

line
t=0

C_0

q^0
a_0

D_1-column

a_0
p^0

p^1
p_0^1

line
t=1

q_0^1
q_0^1

q^0

q_0^1
a_1
p^1

q^1

q_0^1

q^1
a_1
p^1
p_0^1
p_0^1

a_0

D_2-column

a_0
p^0

q_{10}^2
q_{10}^2

p_{10}^2
q_1^2
p_{10}^2

p_0^2
p^1
p_0^1

line
t=2

p_{10}^2
p_1^2
p_{10}^2

q_{10}^2
q_1^2
q_{10}^2

q_0^1
q^1
q_0^1

q^0

a_0

q_0^1
a_1
p^1

q_0^1

p_1^2
p^2
p_1^2

q_1^2
q^2
q_1^2

q^1
a_1
p^1
p_0^1

p_0^1

a_0

q_1^2
a_2
p^2

q_1^2

q_{10}^2

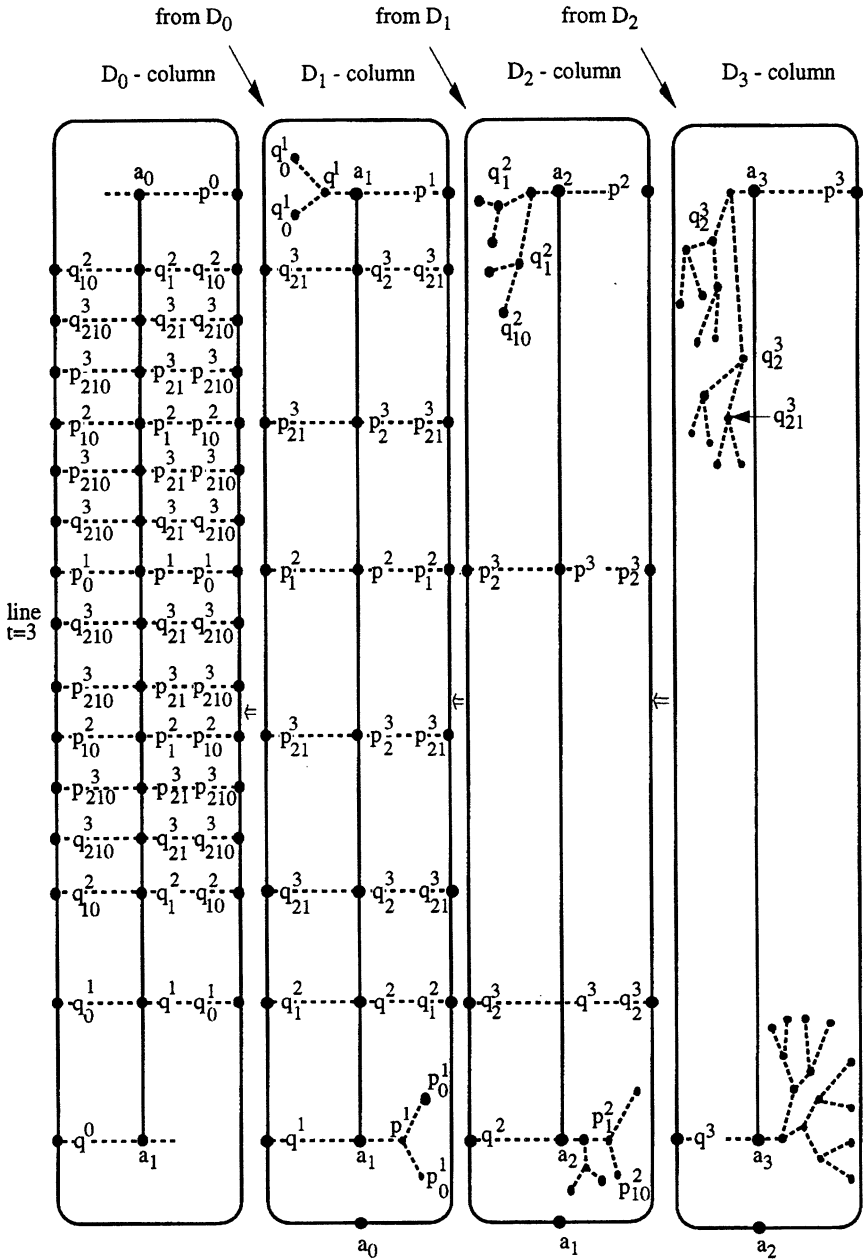q^2
a_2
p_{10}^2
p_1^2

a_1

– 677 –

Fig. 2.9b)   We see here $t = 3$.

We will investigate the set $M_2(g) \cap \Lambda$. Clearly (see remark (A) above) this is exactly the same thing as investigating $M_2(g_1) \cap \Lambda = M_2(g) \cap \Lambda$. So what we will do will be to pick up, with much more details the issues started by figure 2.6 with the help of which we generate figure 2.9. At each time $t = n$ in this figure we have an isomorphism $C_p \approx \partial D_{p+1}$ for all $p + 1 \leq n$. Points on C_p and ∂D_{p+1} which are indicated by the same symbols, have the same image at the source (i.e. they are the same point in K).

Here is the *recursive procedure* for constructing $M_2(g_1) \subset K_1$. At time $t = 0$ we consider $\overline{D}_0$ and $M_2(g_1 \mid \overline{D}_0) \subset \overline{D}_0 \subset K_1$. This is shown on the left upper corner (line $t = 0$, column D_0) of figure 2.9. At time $t = 1$ we consider both $\overline{D}_0$ and $\overline{D}_1$ and we look for $M_2(g_1 \mid (\overline{D}_0 \cup \overline{D}_1))$. The situation on (line $t = 1$, column D_1) is forced by (line $t = 0$, column D_0) which it is imitating (i.e. $M_2(g_1 \mid \overline{D}_1)$ is isomorphic to $M_2(g_1 \mid \overline{D}_0)$); this accounts for the diagonal arrow. But then the situation on (line $t = 1$, column D_1) forces the situation of (line $t = 1$, column D_0) which enriches what we already had at (line $t = 0$, column D_0); this accounts for the horizontal double arrow. (Of course (line $t = 1$, column D_1) contains some extra details with respect to $(t = 0$, column $D_0)$, like the lines (q^1, q_0^1), (p^1, p_0^1) which appear for $(t = 1, D_1)$ but are absent for $(t = 0, D_0)$; these details come from {the double points of g_1 which involve both D_1 and D_0} $\cap D_1$.) Figures 2.9 and 2.9b) (line $t = 3$) suggests how this process continues recursively for all t's. The situation $(t = n, D_n)$ *forces* $(t = n + 1, D_{n+1})$, which then in turn forces $(t = n + 1, D_n)$, $(t = n + 1, D_{n-1})$, ..., $(t = n + 1, D_0)$. Here again $(t = n + 1, D_{n+1})$ contains some extra details with respect to $(t = n, D_n)$. These come from {the double points of g_1 involving both D_{n+1} and $\sum_0^n D_i$} $\cap D_{n+1}$. But these kind of details are completely irrelevant for our main discussion, which focuses on $M_2(g) \cap \Lambda$ and on the set of limit points of $M_2(g) \cap \Lambda$; we will, generally speaking, ignore them hereafter.

For each $t = n$ and $p < n$ the situation on C_p and ∂D_{p+1} are canonically isomorphic, as one can see it in figures 2.9 and 2.9b). Also the various points of $M_2(g_1)$ successively appearing on C_p and/or on ∂D_{p+1} at times $t = 0$, $t = 1$, ... carry some lower indexes and we will define the *flavour* of the respective double point as being

$$\text{flavour} \overset{\text{def}}{=} (\text{the number of lower indexes}) + 1$$

(so that, for instance, flavour$(p^0) = 1$, flavour$(q_{21}^3) = 3$, ...). If $x \in M_2(g) \cap C_p$ and if the flavour of x is q, this means exactly that x, considered

as a point in C_p, is a double point involving D_p and D_{p+q}. Our double points also carry a letter (like p and q) and an upper index, which together, will be called the *colour* of the corresponding double point. Notice that colour and flavour together determine completely the set of indices (upper and lower, with their order, and of course the letter p/q too) which accompany the double point. (But colour does not determine flavour, nor the other way around.) In other words any

$$x \in M_2(g) \cap \left(\sum_0^\infty C_i \right) \approx M_2(g) \cap \left(\sum_0^\infty \partial D_{i+1} \right)$$

is *completely identified* by its combinaison of flavor and colour. The geometric meaning of the lower indexes should also be clear, for intance

$$q^3_{210} = \left\{ \text{the result of the } q^3 \in D_2 \cap \partial D_3 \text{ on } D_1 \text{ and then finally on } D_0 \right\}.$$

The upper index corresponds to the first time t when the double point in question (without its lower indices) appears.

The canonical isomorphism $C_n \approx \partial D_{n+1}$ (see for instance C_0 and ∂D_1 in figure 2.9b)) sends double points to double points with the same colour and flavour (like a $p^3_{21} \in C_0$ to a $p^3_{21} \in \partial D_1$ (fig. 2.9b)).

The important feature of this recursive procedure is the following. Consider two consecutive columns (we will focus from now on D_0 and D_1) after the inductive procedure $(t = 0) \Rightarrow (t = 1) \Rightarrow \cdots$ has been completed, i.e. at time $t = \infty$. Infinitely many horizontal dotted lines passing through points endowed with colour and flavour will be contained now both in $C_0 \subset D_0$ and $C_1 \subset D_1$ (the small irrelevant details like (q^1_0, q^1, q^1_0), (p^1_0, p^1, p^1_0) contained in Int D_1 will be, of course, forgotten from now on). We make the following claims:

Alg-0. — Our whole *infinite* construction is invariant under the *unilateral* shift

$$(t = n, \, D_i) \overset{\text{shift}}{\Longrightarrow} (t = n + 1, \, D_{i+1}) \tag{2.8}$$

as long as colours are ignored. Both *the drawing and the flavours are shift invariant*. Of course, the shift can be accompanied by a precise, well-defined trasformation of the colours which the reader can explicit easily. We also have a colour and flavour conserving monomorphic inclusion map

$$(t = n, \, D_i) \overset{\text{inclusion}}{\Longrightarrow} (t = n + 1, \, D_i). \tag{2.9}$$

Alg-1.— The situation of $(\text{Int }C_0) \cap (\text{horizontal dotted lines})$ at the time $t = \infty$ is exactly the $M_2(g) \cap \Lambda$ we are looking for.

Alg-2.— Before we state the next claim let us notice the following feature which is build into the detailed construction of the figure 2.9 and figure 2.9b. When for a given $t = n$ (like for instance $t = 3$ and for two consecutive columns i, $i+1$ (like for instance D_0 and D_1) two horizontal lines are drawn exactly at the same level (like for instance $[p_{10}^2, p_1^2, p_{10}^2] \subset D_0$ and $[p_{21}^3, p_2^3, p_{21}^3] \subset D_1$) they correspond to the same flavours f for the middle point and $f + 1$ for the two extreme points, i.e. these two lines go from a point of flavour $f + 1$ to another point of flavour $f + 1$ passing through a middle point of flavour f. On the column i the lines in question are in the image of the inclusion (2.9) and all this is consistent with the following "commutative" diagram (which is flavour preserving) but where the left horizontal translation is not colour preserving (see Diagram 1). Actually the p/q part of colour is preserved, but this is irrelevant. Our figures, as far as the horizontal alignement is concerned, have been drawn exactly so as to make the diagram above commutative. This has nothing to do with the $C_i \approx \partial D_{i+1}$ isomorphism. On the other hand the two horizontal lines in question correspond, respectively, to the double points involving {both D_i and D_{i+f}} and/or {both D_{i+1} and D_{i+f+1}}.

(t=n-1,D$_i$)

INCLUSION SHIFT

(t=n,D$_i$) (t=n,D$_{i+1}$)
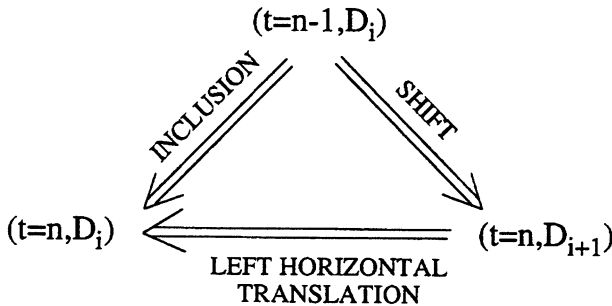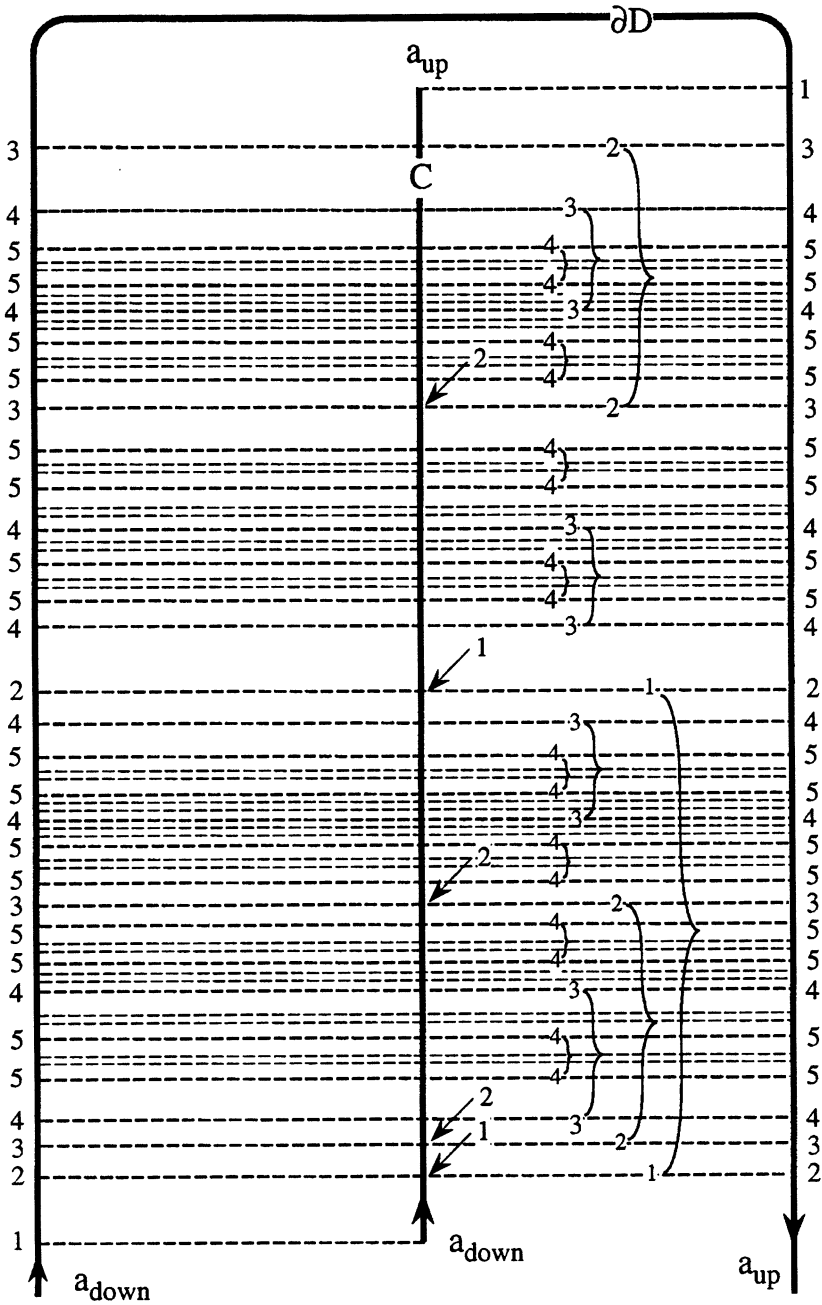
LEFT HORIZONTAL
TRANSLATION

Diagram 1

Fig. 2.10 The dynamical figure $(t = \infty, D)$;

- - - (where no numbers are indicated)= [6, 5, 6]; in order not to make the drawing too messy, most of the symbols 5 and all the 6's are lacking on C and ∂D; for similar reasons, the numbers 1, 2, ..., for the points of C have been shifted to the right, on the same dotted horizontal line; the vertical parenthesis suggests the self similar pattern which this figure starts to build.

Remark. — As already said, the device of drawing at the same horizontal level lines which correspond to each other under (2.9) does not keep track of the flavour (and colour) conserving isomorphism

$$(t = n,\, C_i) \approx (t = n,\, \partial D_{i+1})\,.$$

But it makes possible what comes next.

As a consequence of all this (and this is finally our claim *Alg-2*, if we forget about the colours and keep only the flavours (1, 2, ...) then the figures $(t = \infty,\, D_0)$ and $(t = \infty,\, D_1)$ are canonically isomorphic. Let us call this infinite object $(t = \infty,\, D_0) \approx (t = \infty,\, D_1)$ "the figure $(t = \infty,\, D)$". The isomorphism $(t = \infty,\, D_0) \approx (t = \infty,\, D_1)$ comes, of course, from the shift (2.8). At the level of $(t = \infty,\, D)$ the isomorphism $C_0 \approx \partial D_1$, becomes $C \approx \partial D$ and this isomorphism conserves flavour. We will draw the transversal Λ inside the figure $(t = \infty,\, D)$ and consider

$$F_n \stackrel{\text{def}}{=} \{\text{the double points of } \Lambda \cap M_2(g) \text{ which have flavour } n\}$$

$$= \{\text{the double points of } \Lambda \cap M_2(g) \text{ which come from } gD_0 \cap gD_n\}\,.$$

$$(2.10)$$

Figure 2.10 suggest how one builds, inductively our figure $(t = \infty,\, D)$. The important point is that now we are in the presence of a feedback $C \Leftrightarrow \partial D$ which generates the following.

Dynamical rule for construction $(t = \infty,\, D)$ (and hence the set $\Lambda \cap M_2(g)$)

We start by drawing the bare lines C and ∂D like in figure 2.10. "Bare" means without any details other than their orientations, in particular without any double point of g and/or g_1. Then, as an input we draw the (asymmetrical) horizontal lines $(a_{\text{up}}, 1)$, $(a_{\text{down}}, 1)$. Now ∂D is no longer bare since it contains two points with flavour 1. The rule that there is a *flavour conserving isomorphism* $C \approx \partial D$ forces then, by dynamical self

consistency, two points with flavour 1 on the line C. From these two points we draw horizontals *symmetrically* in both direction until we hit ∂D at four points with flavour 2. By dynamical self-consistency these points have to exist also on C so that

$$(C, \text{ with 1's and 2's}) \approx (\partial D, \text{ with 1's and 2's}).$$

From the points with flavours 2 on C we draw, symmetrically, horizontals which hit ∂D in eight points with flavour 3. By dynamical self-consistency these have to be drawn on C too, and so on.

By now this dynamical process of feedback between C and ∂D should be clear and hence, within the margin of freedom which this construction leaves, we know now our set $\Lambda \cap M_2(g) \approx C_0 \cap M_2(g)$ which comes equipped with an obvious disjoined decompositon

$$\Lambda \cap M_2(g) = F_1 + F_2 + \cdots + F_n + \cdots \qquad (2.10b)$$

where, like in (2.10), we have $F_n = \{$ double points of flavour n, i.e. double points which involve D_0 and $D_n\}$

Remark. — Let us denote by $\partial D \xrightarrow[\approx]{d} C$ the canonical homeomorphism $\partial D \approx C$ and by $\partial D \xrightarrow{h} C$ the not everywhere defined horizontal projection from ∂D to C, so that $C \xrightarrow{h^{-1}} \partial D$ is the double-valued map which attaches to $p \in C$ two points of ∂D sitting on the same horizontal line. With these notations our feedback loop via which the infinite figure 2.10 has been constructed is represented in Diagram 2.
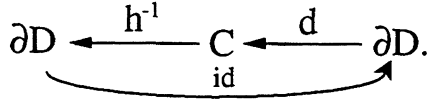
$$\partial D \xleftarrow{\;\;h^{-1}\;\;} C \xleftarrow{\;\;d\;\;} \partial D.$$
$$\underbrace{\phantom{\partial D \xleftarrow{\;\;h^{-1}\;\;} C \xleftarrow{\;\;d\;\;} \partial D}}_{\text{id}}$$

Diagram 2

If we denote generically by $n \in \partial D$ the points with flavour n, then our dynamical rule for building up the $F_1 + F_2 + \cdots$ (as a subset of ∂D) is schematized by the formula

$$1 + \underbrace{h^{-1}d(1)}_{2} + \underbrace{h^{-1}dh^{-1}d(1)}_{3} + \cdots = 1 + W(1) + W^2(1) + \cdots \qquad (2.10c)$$

Here $\partial D \xrightarrow{\quad W \stackrel{\text{def}}{=} h^{-1}d \quad} \partial D$ and, by definition, formula (2.10c) is the "Whitehead algorithm".

In order to analyze $\Lambda \cap M_2(g)$ we go back to the quadratic map from figure 2.1. On the real axis we can see four points $0 < x_0 < y_0 < y_1 < x_1 < 1$ such that $f_\lambda(x_0) = f_\lambda(x_1) = 0$ and $f_\lambda(y_0) = f_\lambda(y_1) = 1$. The following things happen.

LEMMA 2.2

(1) *Our dynamical rule for construction $\Lambda \cap M_2(g)$ is exactly the same as the dynamical rule for constructing the set (see (2.1)):*

$$\mathcal{E} = E \cup f_\lambda^{-1}E \cup f_\lambda^{-2}E \cup \cdots \cup f_\lambda^{-n}E \cup \cdots \subset [0,1], \qquad (2.11)$$

where $E = \{x_0, y_1\}$ and where f_λ is the quadratic map from figure 2.1.

(2) *Whitin the margin or freedom allowed by our construction of the representation*

$$K \underset{g}{\to} Wh^3$$

we can choose g so that:

$$\begin{aligned} \{\text{the set of limit point } \Lambda \cap M_2(g)\} = \\ = \{\text{the Julia set of the quadratic map } f_\lambda\}. \end{aligned} \qquad (2.12)$$

It is well-known that the Julia set in question is a Cantor set. But anyway we also have the following.

(3) *For any choice of g (within the margin of freedom for the construction of $K \underset{g}{\to} Wh^3$) the $\{$set of limit points of $\Lambda \cap M_2(g)\}$ is always uncountable (in fact it always contains a Cantor set).*

Proof. — Before we start constructing the set (2.11) we will redraw the graph of f_λ (or rather the interesting part of this graph) in figure 2.11, which the reader should compare with the bare figure 2.10 (i.e. that figure before the dynamical process starts). On the figure 2.11, we perceive two isomorphisms $\partial D \approx \{\text{graph } f_\lambda\} \xrightarrow{j} A$ given by $j(x, f_\lambda(x)) = x$ and $A \xrightarrow{i} C$ going from $p \in A$ vertically to the diagonal $x = y$ and then to C, via the horizontal projection (see the figure 2.11). Let us denote generically by n the points in A which belong to $f_\lambda^{-(n-1)}E$ (fig. 2.12).
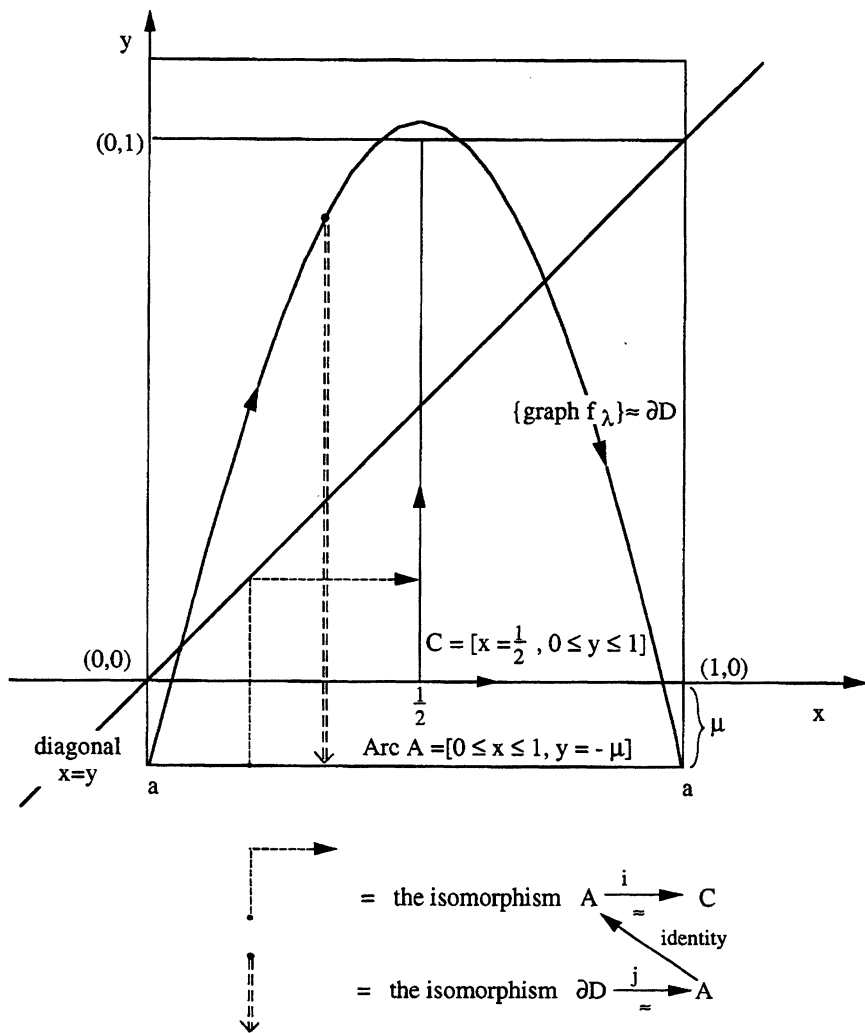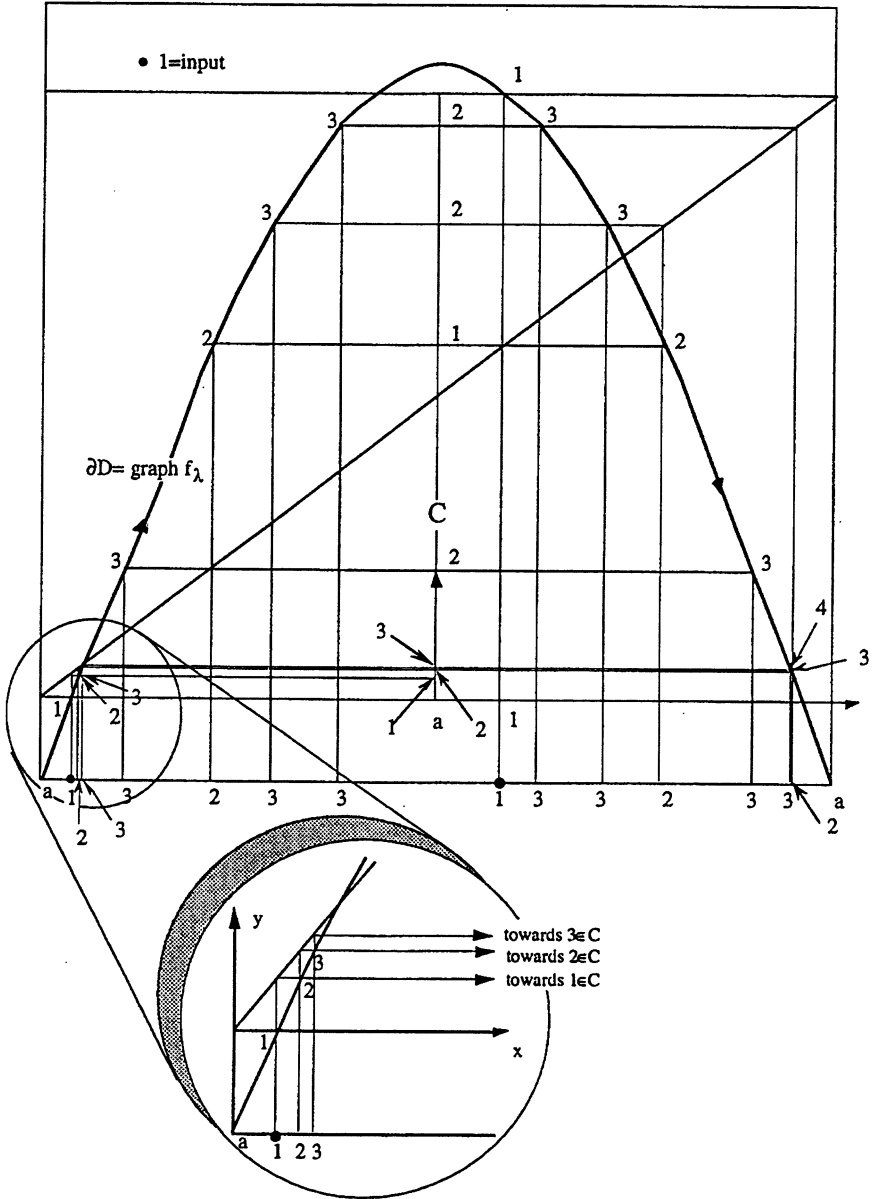
Fig. 2.11 The isomorphism $\partial D \xrightarrow[\approx]{d=i\circ j} C$.

Fig 2.12 In this figure (next page), on the segment A, points marked with 1 are in E, those with 2 in $f_\lambda^{-1}E$, those with 3 in $f_\lambda^{-2}E$, and so one; the dynamical feedback between C and ∂D, in this figure, is exactly the same as in figure 2.10; for typographical reasons this figure differs from 2.1 by a homothety which brings the diagonal closer to the x axis.

In that figure we also have denoted with the same letter n the corresponding points in ∂D via j^{-1}, or in C via i. The dynamics of the transformation

$$ n = f_\lambda^{-(n-1)} E \quad \Longrightarrow \quad f_\lambda^{-n} E = (n+1) $$

can be expressed by the following graphical rules which we can see displayed in figure 2.12.

Go from $n \in A$ to $i(n) \in C$, then draw the horizontal line through $i(n)$, take its two intersection points with $\partial D \approx$ graph f_λ and finally take the images of these intersection points via j back to A. This defines the $\{n+1\} \subset A$. So we can define

$$ \mathcal{J} \overset{\text{def}}{=} jh^{-1}i $$
$$ A \longrightarrow A $$

and passing from ∂D to A via j, we have the obvious commutative diagram

$$
\begin{array}{ccccc}
\partial D & \xrightarrow{\; d=i \circ j \;} & \underset{\text{Whitehead}}{C} & \xrightarrow{\; h^{-1} \;} & \partial D \\
\big\downarrow{\scriptstyle j} & & & & \big\downarrow{\scriptstyle j} \\
A & \xrightarrow{\; i \;} & \underset{\text{Julia}}{C} & \xrightarrow{h^{-1}} \partial D \xrightarrow{j} & A
\end{array}
$$

which means $\mathcal{J}\big(j(x)\big) = jW(x)$ and hence also $\mathcal{J}^p\big(j(x)\big) = jW^p(x)$ for all p's and $x \in \partial D$. This shows that if we start with $j(1) = E$ (where "1" is the same now as in formula (2.10c)) then the "Whitehead algorithm" (2.10c) and the "Julia algorithm"

$$ j(1) + \mathcal{J}\big(j(1)\big) + \mathcal{J}^2\big(j(1)\big) + \cdots $$

are conjugate via $\partial D \xrightarrow{j} A$. In other words via the isomorphism $A \xrightarrow{i} C$, the rule we just have for building (2.11) is exactly the dynamical rule for constructing $(t = \infty, D)$ and hence $\Lambda \cap M_2(g)$; figures 2.10 and 2.12 are basically the same, and with this our (1) is proved.

Notice now that in passing from $t = n - 1$ to $t = n$ via the

$$ (t = n-1, D_0) \quad \overset{\text{inclusion}}{\Longrightarrow} \quad (t = n, D_0) \tag{2.13} $$

(see also (2.9)) one has to add at level $(t = n)$ all the horizontal lines of the form

$$ \left[\ell^n_{i_1 \, i_2 \, \ldots \, i_n}, \; \ell^n_{i_1 \, i_2 \, \ldots \, i_{n-1}}, \; \ell^n_{i_1 \, i_2 \, \ldots \, i_n} \right], \tag{2.13n} $$

with $\ell = p$ or q, which correspond exactly to

$$\{\text{the double points of } g_1 \text{ involving both } D_0 \text{ and } D_n\} \cap D_0, \qquad (2.14)$$

But once $g_1 \mid (D_1 + D_2 + \cdots + D_{n-1})$ has been fixed (and hence also all the lines (2.13) for $i \le n - 1$ we can fix arbitrarily the position of (2.3i) in a compatible way with the already existing situation. This is archieved by an obvious isotopy of $g_1 \mid D_n$, keeping $g_1(\partial D_n)$ fixed. In other words within our allowed margin of maneuver we can realize a homeomorphism $\Lambda \to [\,0\,,1\,]$ sending $\Lambda \cap M_2(g)$ onto $\mathcal{E}$ and preserving the graduation by the n's. This proves (2). Notice that there is no dynamical feedback at the level of this discussion. For the proof of (3) we start by noticing that the points of $\Lambda \cap M_2(g)$, as presented by the dynamical process which accompanies figure 2.10, come naturally in *pairs of points with the same flavour.* (See the vertical curved brackets parallel to C, in figure 2.10.) So we find in C one segment I_1 with (endpoints of) flavour 1, two disjoined segments I_2 with (endpoints of) flavour 2 and generally speaking 2^{n-1} two-by-two disjoined segments I_n with (endpoints of) flavour n. The point (3) from lemma 2.2 is now a consequence of the following.

LEMMA 2.3

(1) The nested system of segments $I_n \subset C$ satisfies the following conditions.

(a) The arc I_1 contains exactly one of the arcs I_2.

(b) Each arc I_2 contains exactly one of the arcs I_3 and as far as the two remaining I_3 arcs are concerned, one is contained in $I_1 - I_2$, the other one is disjoined from $[I_1, I_2]$.

$\vdots$

(n) From the $2^n = \sum_{i=0}^{n-1} 2^i + 1$ arcs I_{n+1}, the first 2^{n-1} are contained each one in an I_n arc, the next 2^{n-2} each one in an I_{n-1} arc but not in I_n, ..., the next 2^i each one in an I_{i+1} arc but not in $I_{i+2} + \cdots + I_n$, ..., and finally, the last one is outside $I_1 + \cdots + I_n$.

$\vdots$

(2) As an immediate consequence of (1), the set of limit points of

$$\Lambda \cap M_2(g) = \{\text{the set of endpoints of the various } I_n\}$$

is uncountable.

Before proving our lemma let us notice that our dynamical rule building the figure 2.10 produces for each n a collection of 2^{n-1} details like the one in figure 2.13a). In passing from n to $n+1$ each of the arcs I_{n+1} gives itself rise to a detail like the one in figure 2.13b). This kind of *self-similarity* which is expressed by (1) is, of course, a well-known feature of *chaotic behaviour*. This remark enhances on (1) in lemma 2.3. The reader will not find it hard to work out in detail the combinatorics of the nested system $\{I_n\}$, including the orientations of the details like the one in figure 2.13a) with respect to C. But the only thing we need in order to get (3) from lemma 2.2 is the numerical estimate from (1) in our present lemma.
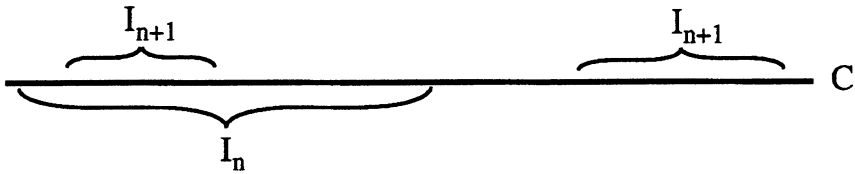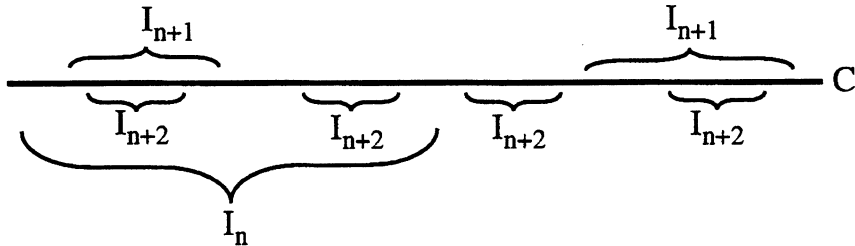

Fig. 2.13a)

Fig. 2.13b)

Proof of the lemma 2.3. — We go back to the context of figure 2.1 and we consider now $E' = \{x_0, y_0\}$ instead of $E = \{x_0, y_1\}$. Our first claim is that the dynamical rule for constructing our $\Lambda \cap M_2(g)$ is exactly the same as the one for producing

$$E' \cup f_\lambda^{-1} E' \cup f_\lambda^{-2} E' \cup \cdots \cup f_\lambda^{-n} E' \cup \cdots \qquad (2.15)$$

This can be shown exactly like in the proof of (1) from lemma 2.2. We will deduce the combinatorics of (2.15) (and hence the combinatorics of (2.11), i.e. of our $\Lambda \cap M_2(g)$) from the much easier combinatorics of

$$E'' \cup f_\lambda^{-1} E'' \cup f_\lambda^{-2} E'' \cup \cdots \cup f_\lambda^{-n} E'' \cup \cdots \qquad (2.16)$$

where $E'' = \{x_0, y_0, y_1, x_1\}$. Just like $\Lambda \cap M_2(g)$, i.e. like (2.11) or (2.15), the set (2.16) can be described by a system of nested intervals $\ldots, J_n, J_{n+1}, \ldots$ If we denote by A_1 and A_2 the arcs $A_1 = f_\lambda[x_0, y_0]$, $A_2 = f_\lambda[y_1, x_1]$ then a typical J_n has the form

$$J_n = f^{-n}(A_{i_n}) \cap f^{-n+1}(A_{i_{n-1}}) \cap f^{-1}(A_{i_1}) \cap A_{i_0}, \qquad (2.17)$$

where $i_1, i_2, \ldots, i_n \in \{1, 2\}$. This means that now there are 2^n arcs J_n and each J_n contains exactly two J_{n+1}'s. One obtains the system $\{I'_n\}$ attached to (2.15) from the system $\{J_n\}$ by eliminating, individually, each J_n which is such that $i_n = 2$ (see (2.17)). This changes something like figure 2.13c) into 2.13a). This proves lemma 2.3 and hence also finishes the proof of lemma 2.2.
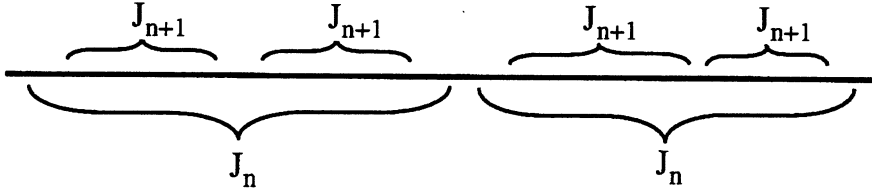

Fig. 2.13c)

Comments

(I)   We make the following *conjecture*.

CONJECTURE .—   *Consider any arborescent representation of the form*

$$X \xrightarrow{\varphi} Wh^3 .$$

for the Whitehead manifold. One can always find smooth tight transversals $\Lambda \subset X$ *to* $M_2(\varphi)$ *such that the set of limit points of* $\Lambda \cap M_2(\varphi)$ *is uncountable.*

We conjecture actually that the situation we have just analyzed is the *best* possible as far as $\Lambda \cap M_2(\varphi)$ is concerned.

Of course, if we move from Wh^3 to a highly *non-aspherical*

$$(Wh)_h^3 = Wh^3 - \bigcup_{n=1}^{\infty} C_n$$

(see formula (1.3)) then the representation theorem provides us with *almost arborescent* representations

$$Y \xrightarrow{\psi} (Wh)_h^3,$$

where the set of limit points of $\Lambda \cap M_2(\psi)$ is finite. In the other words, via redundency we can get rid of the chaotic behaviour.

(II) It has been speculated by several people that there is a connection between exotic low-dimensional topology and chaotic dynamical systems (see for instance the first lines in chapter 6 of [FL]). Our previous discussion is a hint of possible connections between wild open 3-manifolds and real 1-dimensional dynamics. This might be part of a more general picture: John Hubbard conjectures that complex 2-dimensional (or already complex 1-dimensional?) dynamics can be connected to wild behaviour in 4-dimensional differential topology, in particular to the fake R^4's [FL]. Here is a more precise conjecture of John Hubbard.

Consider the Hénon map $\mathbb{C}^2 \xrightarrow{H} \mathbb{C}^2$:

$$\begin{pmatrix} x \\ y \end{pmatrix} \xrightarrow{\ H\ } \begin{pmatrix} x^2 + c - ay \\ x \end{pmatrix}$$

with precisely tuned values of the parameters a, c (like for instance $c = 0$, $a = 0$, 3) so that H has an attractive fixed point with a basin U for which there is a biholomorphic surjection $\mathbb{C}^2 \xrightarrow{L} U$ conjugating H to the linear part at the fixed point).

CONJECTURE .— *The manifold* $\varinjlim (\mathbb{C}^2, L)$, *produced by glueing the n'th $\mathbb{C}^2$ to the $(n+1)$'th $\mathbb{C}^2$ via $\mathbb{C}^2 \xrightarrow[\approx]{L} U \subset \mathbb{C}^2$ is a nonstandard $\mathbb{C}^2$ (from the analytic standpoint).*
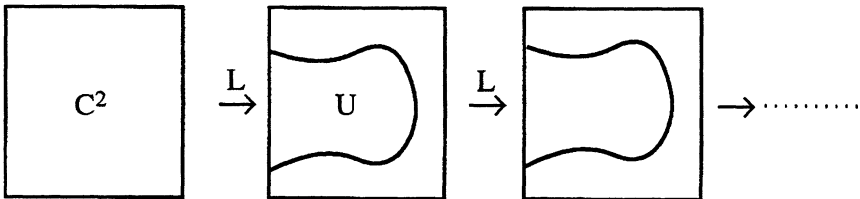

Fig. 2.14

(III) The kind of dynamics which appears in this paper is the relatively simple dynamics $z \rightarrow z^2 + c$ with c outside the Mandelbrot set (which is also akin to the Smale horseshoe, see figure 2.15).
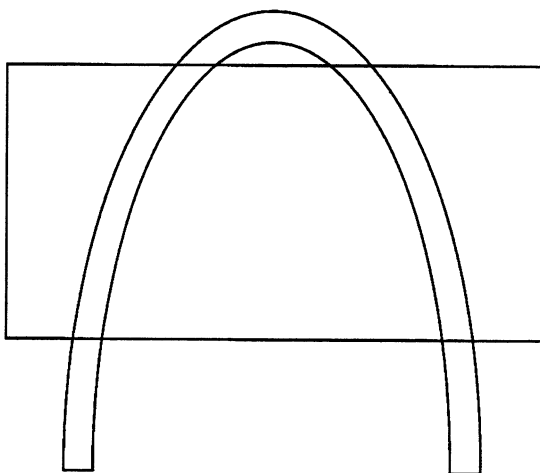
Fig. 2.15

Is there also a topological role for the more subtle dynamics $z \to z^2 + c$ with c inside the Maldebrot set and/or for something like the Hénon map?

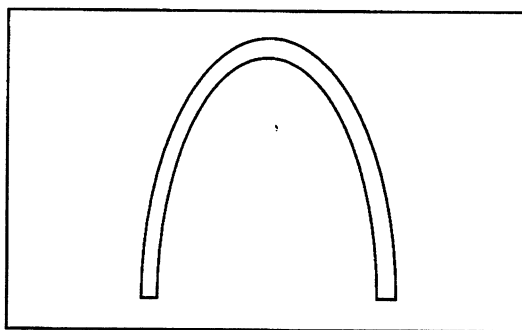**Fig. 2.16**   Schematical view of the Hénon map.

(IV)   Here is an explicit conjecture of John Hubbard. We consider the following map $\mathbb{C}^2 \to \mathbb{C}^2$

$$\begin{bmatrix} x \\ y \end{bmatrix} \longrightarrow \begin{bmatrix} x^2 - cy^2 + x^3 \\ y^2 \end{bmatrix}$$

which has 0 as an attractive fixed point.

CONJECTURE (John Hubbard) .— *For any c on the boundary of the Mandelbrot set the basin of 0 is a nonstandard R^4. Moreover, for distinct c's these manifolds are distinct.*

Bibliography

[B] BLANCHARD (P.) . — *Complex analytic dynamics on the Riemann sphere*, B.A.M.S. **11**, n° 1 (1984), pp. 85-141.

[F] FEIGENBAUM (M.) . — *Universal behaviour in nonlinear systems*, Los Alamos Science **1** (1980), pp. 4-27.

[FL] FREEDMAN (M.) and LUO (F.) . — *Selected applications of Geometry to low-dimensional Topology*, Marker Lectures in the Math. Sciences, Princ. Univ. (1989).

[Po1] POÉNARU (V.) . — *Infinite processes and the 3-dimensional Poincaré conjecture 1 – The collapsible pseudo-spine representation theorem*, Topology **31** (1992), pp. 625-636.

[Po2] POÉNARU (V.) . — *Representations of open simply connected 3-manifolds, a finiteness result*, Prépublication d'Orsay (1992).

[R] ROLFSEN (D.) . — *Knots and Links*, Math. Lect. Series (1976).

[S] SMALE (S.) . — *Differentiable dynamical systems*, Bull. A.M.S. **73**, n° 6 (1967), pp. 747-817.